ACADEMIC PRESS

Available online at www.sciencedirect.com
SCIENCE DIRECT®

Molecular and Cellular Neuroscience 24 (2003) 489–502

MCN Molecular and Cellular Neuroscience

www.elsevier.com/locate/ymcne

Inhibition of CDK5 is protective in necrotic and apoptotic paradigms of neuronal cell death and prevents mitochondrial dysfunction

Jochen H. Weishaupt,[a] Lothar Kussmaul,[b] Philipp Grötsch,[a] Armin Heckel,[b] G. Rohde,[a] H. Romig,[b] Mathias Bähr,[a*] and Frank Gillardon[b]

[a] *Department of Neurology, University Hospital Göttingen, Robert-Koch-Strasse 40, 37075 Göttingen, Germany*
[b] *Boehringer Ingelheim Pharma KG, Binger Strasse 173, 55216 Ingelheim, Germany*

Received 22 January 2003; revised 15 May 2003; accepted 19 May 2003

Abstract

Previous studies suggested that pro-apoptotic stimuli may trigger a fatal reactivation of cell cycle elements in postmitotic neurons. Supporting this hypothesis, small molecule inhibitors of cyclin-dependent kinases (CDKs), which are known primarily as cell cycle regulators, are neuroprotective. However, available CDK inhibitors cannot discriminate between the different members of the CDK family and inhibit also CDK5, which is not involved in cell cycle control. Testing a new class of CDK inhibitors, we find that inhibitory activity against CDK5, but not cell cycle-relevant CDKs, confers neuroprotection. Moreover, we demonstrate that cleavage of the CDK5 activator protein p35 to p25 is associated with CDK5 overactivation after focal cerebral ischemia, but not in other models used in this study. We find that blocking CDK5 activity, but not caspase inhibition, protects mitochondrial integrity of lesioned neurons. Thus, in our models, CDK5, rather than cell cycle-relevant CDKs, activates neuronal cell death pathways upstream of mitochondrial dysfunction, and inhibition of CDK5 may promote functional long-term rescue of injured neurons. Moreover, we present the first CDK5-selective small molecule inhibitor, lacking unwanted cytostatic effects due to cross-inhibition of mitotic CDKs.

Introduction

Apoptosis (programmed cell death) is an evolutionary conserved program which has crucial functions during development in controlling the cell number and morphology of multicellular organisms. However, evidence has accumulated that the same apoptotic machinery can be reactivated in the adult organism and contribute to the neuronal cell death of neurodegenerative diseases (Kermer et al., 1999; Reed, 2000).

It has been postulated that apoptosis of postmitotic cells is the result of an abortive and fatal attempt of these cells to reenter the cell cycle on pro-apoptotic stimulation (Heintz, 1993; Rubin et al., 1994). In the past few years, upregulation or activation of components of the cell cycle machinery [e.g., cyclin D1, cyclin-dependent kinases (CDKs), E2F1] has indeed been reported in various models of neuronal cell death (Freeman et al., 1994; Park et al., 1996; Padmanabhan et al., 1999; O'Hare et al., 2002). Only in a few instances, as in the Alzheimer's disease-related model, have neurons entering S phase been described (Copani et al., 1999).

A focus in this field of research is cyclin-dependent kinases, which are important regulators of the cell cycle machinery. An exception is CDK5, which belongs to the family of CDKs and has also been termed neuronal CDK1-like kinase, but is not involved in cell cycle control (Meyerson et al., 1992; van den Heuvel and Harlow, 1993). Much of the functional evidence for the contribution of incomplete cell cycle reentry, or at least reactivation of mitotic CDKs, to neuronal cell death came from the use of small molecule inhibitors of CDKs, such as olomoucine, roscovitine, and flavopiridol (Walker, 1998). These compounds exert neuroprotective effects in vitro and in vivo (Park et al., 1996; Osuga et al., 2000). However, it turns out that these so-called cell cycle inhibitors also strongly inhibit CDK5 (Leclerc et al., 2001), leaving open the possibility that

* Corresponding author. Fax: +49-551-398405.
E-mail address: mbaehr@gwdg.de (M. Bähr).

1044-7431/03/$ – see front matter © 2003 Elsevier Inc. All rights reserved.
doi:10.1016/S1044-7431(03)00221-5

CDK5 could, at least in some experimental paradigms, also be involved in neuronal cell death. Its known physiological substrates have been implicated in cytoskeletal organization, neuronal migration, axonal transport, and neurite outgrowth (Tsai et al., 1993; Nikolic et al., 1996; Chae et al., 1997; Paglini et al., 1998; Zukerberg et al., 2000; Floyd et al., 2001). In contrast to other CDK family members, CDK5 is upregulated during neuronal development (Tsai et al., 1993). Despite its ubiquitous expression, CDK5 activity is almost completely restricted to the central nervous system (CNS), because the CDK5 activators p35 and p39, functional homologues of the cyclins, are specifically expressed in neurons (Tang et al., 1995).

Subcellular redistribution and overactivation of CDK5 in Alzheimer's disease or amyotrophic lateral sclerosis (ALS) supports a role for this kinase in the pathogenesis of neurodegenerative diseases (Patrick et al., 1999; Nguyen et al., 2001). It has been shown that amyloid-β toxicity induces calpain-mediated cleavage of p35 to p25, which is followed by redistribution and overactivation of CDK5 after association with p25 (Lee et al., 2000). Moreover, dominant-negative CDK5 mutants prevent amyloid-β-mediated neurodegeneration in vitro (Lee et al., 2000).

In the present study we provide evidence that, at least under the experimental conditions we investigated and possibly depending on the type of death stimulus, CDK5 inhibition, rather than blocking the cell cycle-relevant CDK1, -2, or -4, protects against neuronal cell death by necrosis and apoptosis. We show that CDK5 acts early in the apoptotic- and necrotic-like neuronal cell death pathways investigated in this study, and inhibition of CDK5 is mitochondrio-protective. Therefore, CDK5 inhibition may promote functional long-term rescue of severed CNS neurons. Finally, we present the first small molecule inhibitor that shows preferred activity toward CDK5. This compound does not have unwanted cytostatic effects due to cross-inhibition of cell cycle-promoting CDKs, and might turn out to be a valuable therapeutic tool in the treatment of neurodegenerative diseases.

Results

Small molecule cyclin-dependent kinase inhibitors that allow differentiation between different CDK family members

Small molecule kinase inhibitors, derived from indolinones, were synthesized at Boehringer Ingelheim Pharma KG, Ingelheim, Germany. Three compounds, termed indolinones A–C, were originally screened for their inhibitory activity against cell cycle-promoting CDK1, -2, and -4 for treatment of tumors (see Experimental methods). Following the first results of our cell culture experiments described below, high-throughput screening for CDK5 inhibitors was performed by scintillation proximity assay, leading to the discovery of indolinone D.

Table 1
C_{50} of indolinones A–D for recombinant CDK1, -2, -4, and -5

IC_{50} (μM)				
	Indolinone A	Indolinone B	Indolinone C	Indolinone D
CDK1	0.025	2.5	0.009	1.0
CDK2	0.036	2.0	0.093	1.1
CDK4	0.0001	0.0008	>10.0	1.0
CDK5	0.005	1.4	1.9	0.067

By use of purified, recombinantly expressed CDKs, it was shown that indolinone A strongly inhibits CDK5 (at least 280- and 380-fold differences in the IC_{50} for CDK5 compared with indolinones B and C) (Table 1), and CDK4, and, to a lesser extent, CDK1 and -2. Indolinones B and C do not inhibit CDK5, but only the cell-cycle-promoting CDK4 (indolinone B) and CDK1 and -2 (indolinone C) in the low nanomolar or subnanomolar range (Table 1). Finally, indolinone D, which was identified in a search for CDK5 selective inhibitors, was confirmed to be a compound with preferred activity against CDK5 (Table 1). Typical sigmoid dose–response-curves of indolinones A–D are shown in Fig. 1. Additionally, inhibition of endogenous CDK5 immunoprecipitated from E18 rat brain lysates by indolinone A is shown in Fig. 2b.

Increasing the concentration of ATP shifted the dose–response curve of indolinone A to the right, demonstrating that this compound class competes with ATP for binding by cyclin-dependent kinases. An ATP-competitive mechanism of action is also supported by co-crystallization studies, demonstrating that a structurally related indolinone localizes to the ATP binding pocket of CDK2 (data not shown). Importantly, all compounds up to 1 μM did not significantly inhibit the in vitro activity of various recombinantly expressed kinases that appear to be involved in neuronal cell death, such as SAPK1c/JNK1, SAPK2a/p38, and MKK1, or kinases that contribute to neuronal survival, e.g., PKBα/Akt and PKCα (data not shown).

Protection against neuronal necrosis correlates with inhibition of CDK5

The cell cycle theory of neuronal cell death postulates that death stimuli trigger an abortive and fatal cell cycle reentry in postmitotic neurons. Therefore, we initially tested indolinones A, B, and C with respect to their neuroprotective efficacy, as they block CDKs essential for cell cycle promotion (Table 1). To demonstrate that our compounds cross cell membranes, are biologically active, and inhibit cell cycle progression in intact cells, we used SKUT-1B uterine tumor cells (Bamberger et al., 1997). As expected based on the results of our in vitro kinase assays described above, both indolinones A and B completely blocked pro-

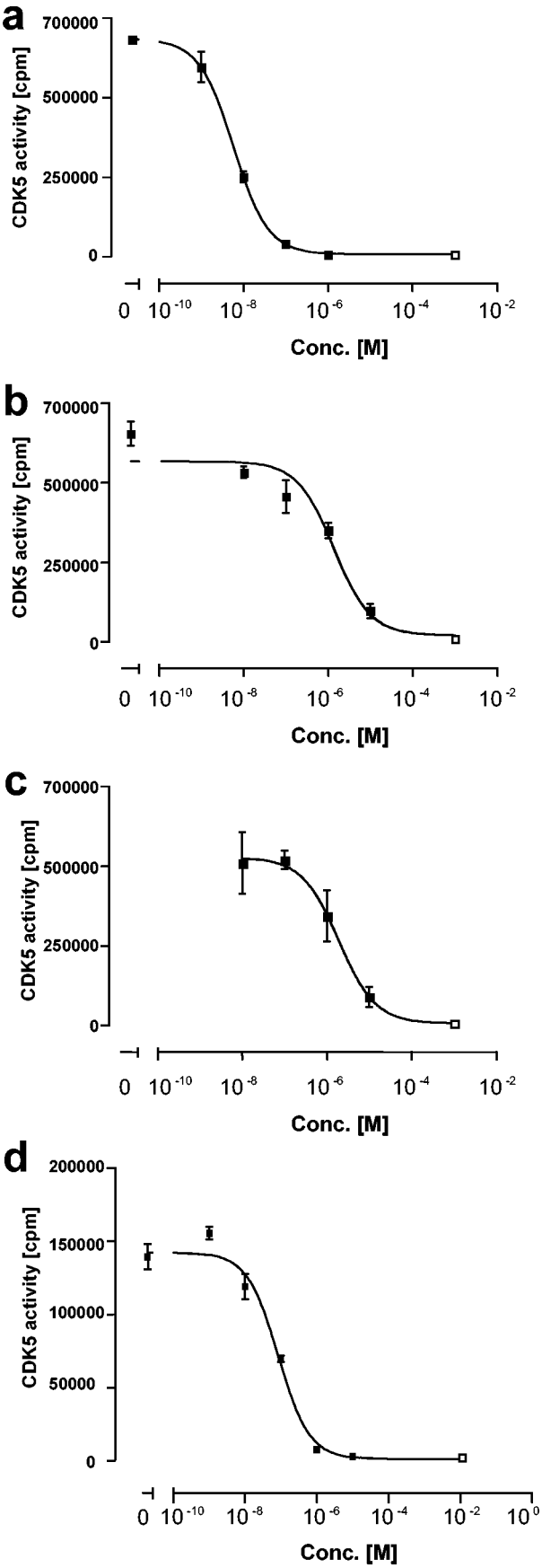

liferation of this cell line with EC_{50} values of 21 and 77 nM, respectively, as assessed by MTT assay.

There is ample evidence that oxidative stress is involved in both acute and chronic neurodegenerative diseases. However, data on a possible role of CDKs in neuronal cell death induced by oxidative stress are lacking. Therefore, we tested our compounds in cultures of cerebellar granule neurons (CGNs) following administration of buthionine sulfoximine (BSO), an irreversible inhibitor of glutathione synthase, which induces delayed neuronal cell death by cellular glutathione depletion and subsequent free radical stress (Wüllner et al., 1999) (Table 2). Indolinone A prevented the decline in Alamar blue fluorescence as a measure of mitochondrial activity with an EC_{50} of 133 nM after 36 h of BSO exposure (Fig. 2a, Table 2). Roscovitine (30 μM), which blocks CDK-1, -2, and -5, but not CDK-4 or GSK-3β (Walker, 1998), completely inhibited the decline in Alamar blue reduction as well (data not shown). At the same time point, we did not observe a BSO-induced increase in nucleosomal DNA fragmentation, indicating the absence of apoptotic DNA cleavage (Fig. 2b). The irreversible, broad-spectrum caspase inhibitor zVAD-fmk (100 μM) did not prevent BSO-induced neurodegeneration, further suggesting that cell death was not mediated via apoptosis. Apoptotic DNA fragmentation became evident at 60 h in indolinone A-treated cultures, however, where mitochondrial activity was still preserved (Figs. 2c, d), indicating a shift from necrosis to apoptosis under sustained free radical stress. The neuroprotective effect of indolinone A was not mediated via scavenging of reactive oxygen species following glutathione depletion, since indolinone A up to 1 μM did not prevent the BSO-induced increase in dichlorodihydrofluorescein fluorescence (7734 $\pm$ 153, 16150 $\pm$ 168, and 14770 $\pm$ 299 fluorescence arbitrary units in sham-treated control cultures, CGNs exposed to BSO and vehicle, and CGNs treated with BSO plus indolinone A, respectively).

Suprisingly, indolinones B and C did not prevent BSO-induced necrosis of CGNs (Table 2). These compounds strongly inhibit the cell cycle-relevant CDK4 or CDK1 and -2, respectively (Table 1), and block tumor cell proliferation as mentioned above, but do not block recombinant CDK5 in a filter plate assay.

As blockade of CDK5, but not cell cycle-promoting CDKs, appeared to correlate with the neuroprotective effectiveness of indolinones A–C in our cell culture models, the compound pool (approximately 616,000 compounds) was screened for inhibitors with preferred activity against CDK5. High-throughput screening by scintillation proximity assay led to the discovery of indolinone D, which ex-

Fig. 1. Inhibition of CDK5 by indolinones a–d in a filter plate assay. Typical sigmoid dose–response curves of indolinone A (a), indolinone B (b), indolinone C (c), and indolinone D (d) are shown. Purified recombinant CDK5, [γ-^{33}P]ATP, and histone H1 as substrate were used to assess CDK5 inhibition (see Experimental Methods). Open symbols represent background controls without histone H1 and test compounds.

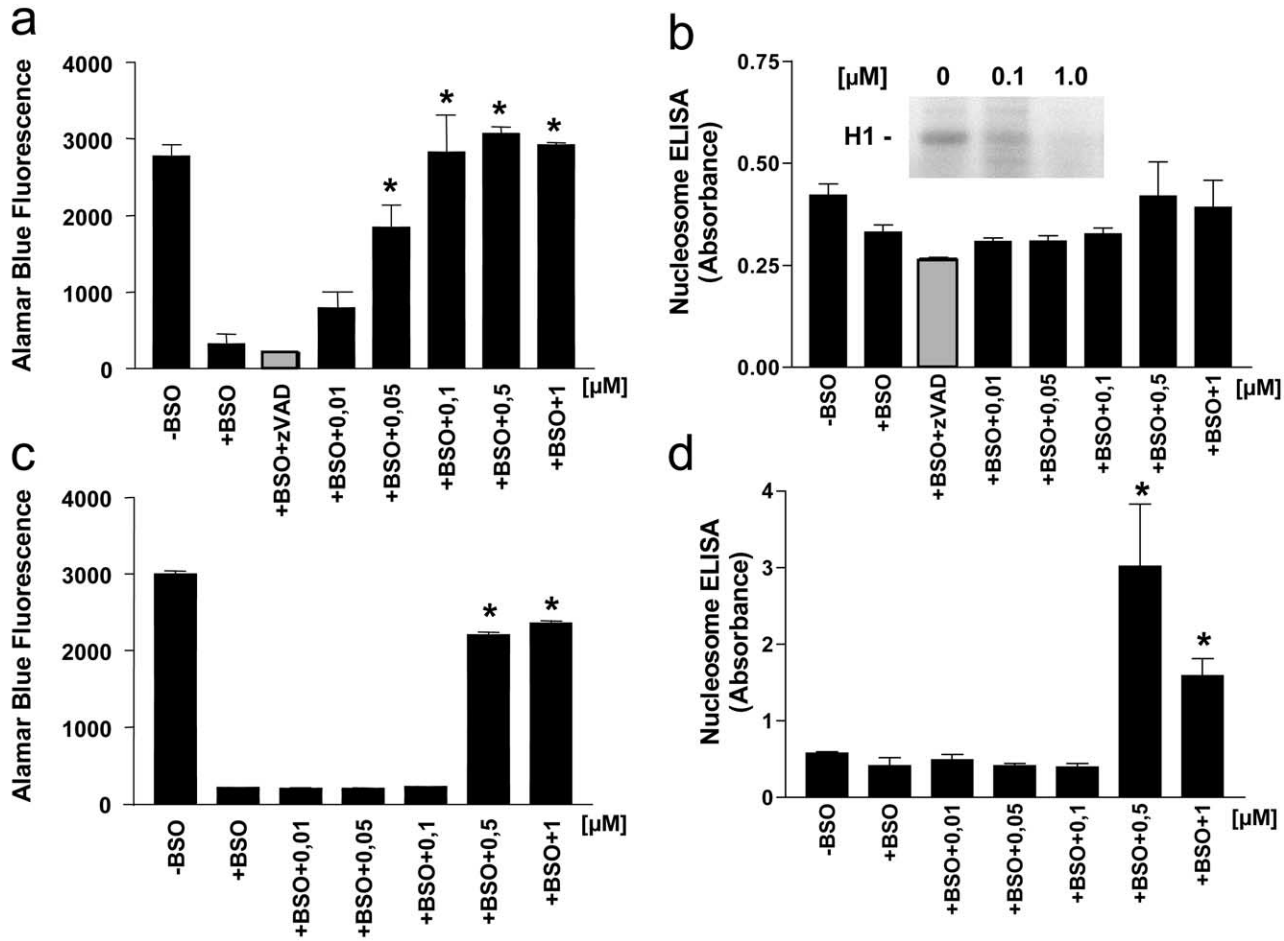

Fig. 2. CDK5 inhibition prevents necrotic cell death in cerebellar granule neurons. Effects of CDK5 inhibition after blockade of glutathione synthesis by buthionine sulfoximine (BSO) and subsequent free radical stress. Indolinone A dose-dependently reduces the decrease in Alamar blue fluorescence as a measure of mitochondrial viability 36 h (a) and 60 h (c) following BSO administration. The caspase inhibitor zVAD-fmk (100 μM) is ineffective (a, b). Alamar blue fluorescence is given in arbitrary units. BSO alone does not lead to apoptotic DNA fragmentation as indicated by nucleosome ELISA after 36 h (b), whereas CGNs protected from BSO-induced mitochondrial dysfunction (c) undergo delayed apoptosis after 60 h (d). Inset in (b): Inhibition of endogenous CDK5 immunoprecipitated from E18 rat brain lysates by indolinone A using histone H1 (H1) as substrate.

hibits improved selectivity against CDK5 (Table 1). In contrast to indolinones A–C, indolinone D did not inhibit proliferation of SKUT-1B uterine tumor cells, demonstrating that this compound, in line with its pharmacological profile, does not impair cell cycle functions. Confirming our previous results and further suggesting that CDK5 inhibition is necessary and sufficient for neuroprotection, indolinone D prevented BSO-induced neuronal necrosis with an EC_{50} of 270 nM (Table 2).

Table 2
C_{50} of indolinones A–D in various neuronal cell death paradigms

EC_{50} (μM)[a]	Indolinone A	Indolinone B	Indolinone C	Indolinone D
BSO[b]	0.133	>1.0	>1.0	0.270
(−) K^+/serum	0.076	>1.0	>1.0	0.120
STS	0.079	>1.0	n.d.	n.d.
(−) Neurotrophin	0.051	>0.3	n.d.	0.053

[a] EC_{50} was calculated from Alamar blue assay (*BSO*), nucleosome ELISA (*STS*, *(−) K^+/serum*) or cell survival indicated by MTT^+ staining (*(−) neurotrophin*).

[b] BSO, buthionine sulfoximine exposure of cerebellar granule neurons; *(−) K^+/serum*, potassium/serum deprivation; *STS*, staurosporine treatment; *(−) neurotrophin*, neurotrophic factor deprivation of immunopurified rat retinal ganglion cells.

Activation of CDK5, but not p35 cleavage, after treatment of CGNs with BSO

As inhibitory activity against CDK5, but not cell cycle-promoting CDKs, appeared to be associated with the neuroprotective effectiveness of indolinones A–D in our cell culture models, we assessed whether CDK5 became overactivated in BSO-treated CGNs. CDK5 was immunoprecipitated from cell lysates and CDK5 activity assays were performed. Densitometric analysis revealed a significant increase in CDK5 activity to 133 ± 11% ($n = 3$) compared with vehicle-treated control cultures.

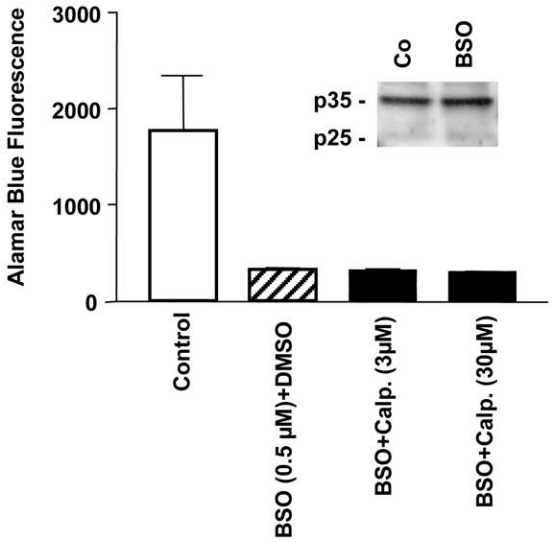

Fig. 3. p35 is not cleaved and calpeptin not protective following glutathione depletion. Calpain inhibition by calpeptin does not protect CGNs exposed to buthionine sulfoximine (BSO) for 36 h from a decrease in Alamar blue fluorescence as a measure of mitochondrial viability. Alamar blue fluorescence is given as arbitrary units. Inset: Representative Western blot, showing that the p35-to-p25 ratio does not change following exposure of CGNs to BSO. Co, control cultures without BSO treatment.

The protease calpain has been shown to induce CDK5 overactivation by cleavage of the CDK5 activators p35 to p25 in other paradigms (Lee et al., 2000). However, we did not detect any change in the ratio of p35 to p25 or in the overall amounts of these proteins in BSO-treated CGNs by Western blot analysis (Fig. 3). In line with this finding, treatment with calpeptin, an inhibitor of calpain, did not prevent the decrease in Alamar blue fluorescence, a measure of mitochondrial function, or death of CGNs following exposure to BSO (Fig. 3).

CDK5-inhibiting indolinones A and D, but not compounds blocking CDK1, -2, or -4, are protective in apoptotic-like models of neuronal cell death in vitro

The neuroprotective efficacy of CDK inhibitors has been described mainly in neuronal apoptosis induced by growth factor deprivation (O'Hare et al., 2002). Indolinones A–D were tested in apoptotic cell death induced by staurosporine treatment or potassium/serum deprivation of CGNs for 24 and 48 h, respectively, and trophic factor deprivation of immunopurified retinal ganglion cells (RGCs) for 48 h. Administration of both indolinones A and D significantly promoted neuronal survival. We obtained submicromolar EC_{50} values for the inhibition of nucleosomal DNA fragmentation (CGNs) or the decrease in MTT-positive RGCs (Table 2).

Calcein and EthD-1 staining clearly demonstrated an enhanced number of surviving CGNs exposed to staurosporine and indolinone A (1 μM) compared with staurosporine alone. Importantly, indolinone A not only preserved cell counts but also prevented neurite fragmentation in staurosporine-treated cultures. The survival-promoting effect of the irreversible pan-caspase inhibitor zVAD-fmk (100 μM) did not approach the effect of indolinone A (Figs. 4a–d).

Again, as in the case of BSO-induced necrosis of CGNs, the CDK-1, -2, and -4-inhibiting indolinones B and C were also not effective against apoptotic death of CGNs and RGCs in the paradigms described above (Table 2).

Effect of CDK inhibition on the survival of axotomized RGCs in vivo

Next we tested the effect of indolinones A and B on the survival of rat RGCs after transection of the optic nerve. This paradigm represents a widely accepted in vivo model for neuronal apoptosis in the CNS. Transection of the optic nerve results in axotomy of RGCs, and intravitreal injection allows application of therapeutic compounds directly to the lesioned neurons. As shown earlier, both p35 and CDK5 are expressed in adult rat RGCs (Hirooka et al., 1996).

Indolinone A, intravitreally injected on Days 0, 4, 7, and 10 after transection of the optic nerve, was highly effective against apoptosis of axotomized RGCs. We found a dose-dependent rescue effect, with up to about threefold more surviving RGCs (1475 $\pm$ 62.8 RGCs/mm^2 retina) (Figs. 5b, d) 14 days after optic nerve transection compared with vehicle control (592 $\pm$ 19.6 RGCs/mm^2) (Figs. 5a, d) or indolinone B treatment (476 $\pm$ 48.3 RGCs/mm^2) (Figs. 5c, d).

We injected 2 μl indolinone A at concentrations of 0.03, 0.15, 0.75, and 3.75 mM, which, according to earlier experience (Klöcker et al., 1998; Kermer et al., 2001), can be expected to result in concentrations at RGCs covering the EC_{50} values of indolinone A for RGCs in vitro (Table 2). Although a plateau effect was not reached at the highest concentration, we could not further increase the concentration of indolinone A due to its limited solubility in water/DMSO. Because indolinone B is even more lipophilic than indolinone A, the highest dose used to test indolinone A could not be reached with indolinone B. For the same reason, we could not test indolinone D.

By Western blot analysis, we did not find evidence of increased conversion of p35 to p25 in rat retina within the first 1 to 4 days of optic nerve transection (data not shown). By immunohistochemistry, we were able to detect the p35 homologue p39 in adult rat RGCs. However, neither by immunohistochemistry and subsequent laser scanning microscopy, nor by Western blot analysis, could we demonstrate any change in its expression or subcellular localization after axotomy (data not shown).

Counteracting CDK5 overactivation reduces infarct volume after transient middle cerebral artery occlusion in rats

Intracerebroventricular (icv) infusion of the pan-CDK inhibitor flavopiridol has recently been demonstrated to reduce

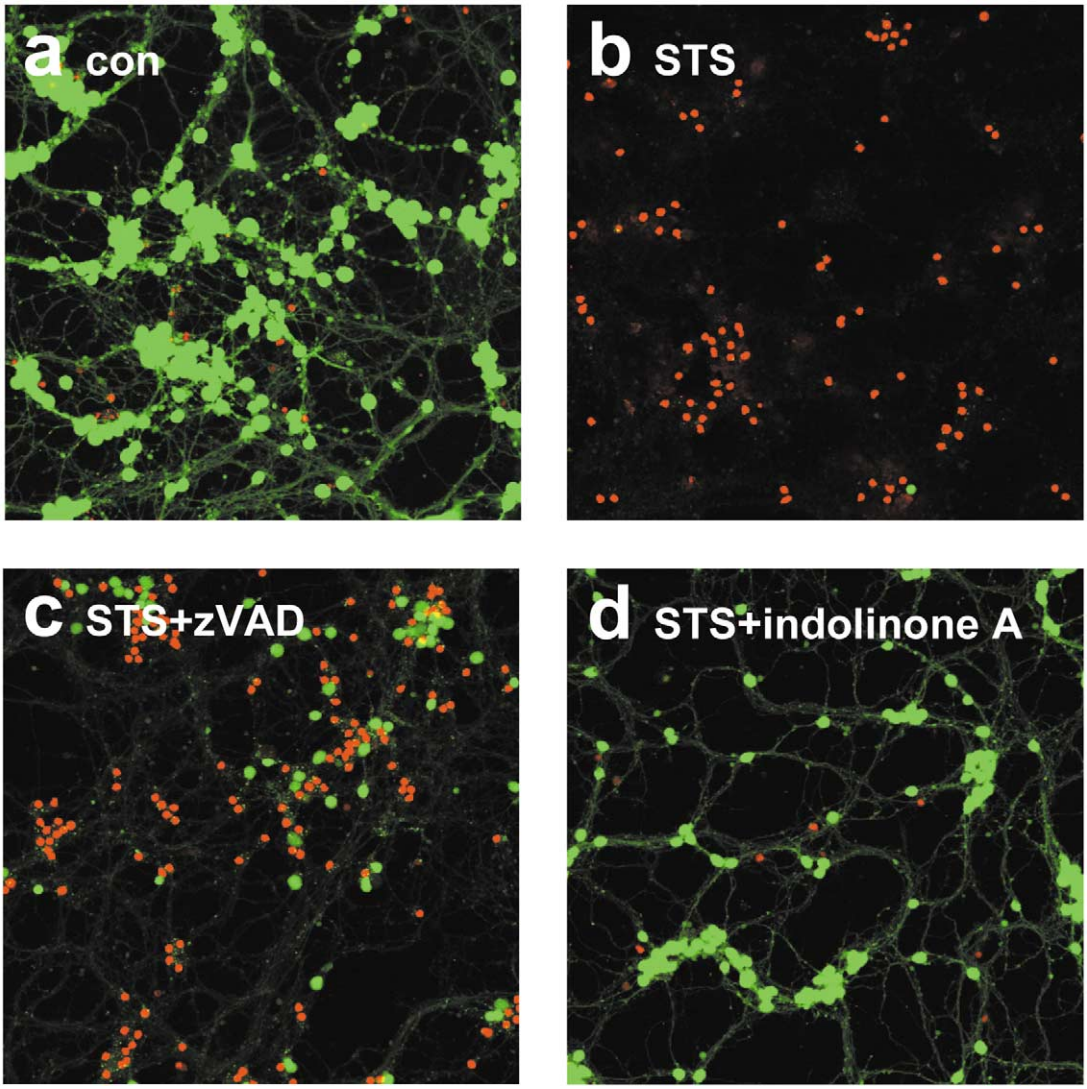

Fig. 4. Increased number of surviving CGNs exposed to staurosporine under indolinone A treatment. (a) Control CGN culture showing intense green fluorescent calcein staining. The nonfluorescent, cell-permeant calcein acetoxymethyl ester is hydrolyzed by intracellular esterases in viable cells, yielding the green fluorescent, polyanionic calcein. (b) Staurosporine (*STS*, 1 μM) induces cell death, indicated by nuclear staining with the red fluorescent ethidium homodimer (EthD-1), which enters only cells with damaged plasma membranes, and concomitant loss of green calcein staining. (c) Moderate survival-promoting effect of caspase inhibition by zVAD-fmk (*zVAD*, 100 μM). (d) Profound neuroprotective effect of indolinone A treatment (1 μM).

infarct volume in rats (Osuga et al., 2000). Suggesting an involvement of CDK5 in ischemic neuronal cell death, we found that at both 4 and 16 h after reperfusion, p35 was cleaved to p25 in protein extracts from the ischemic brain hemisphere following transient (2 h) occlusion of rat medial carotid artery (MCA) (Fig. 6a). This resulted in a significant increase in CDK5 activity to 203 ± 27% (mean ± SEM, $n = 4$), as assessed by CDK5 immunoprecipitation and kinase assay (Fig. 6c), although the amount of CDK5 protein slightly declined in the ischemic hemisphere (Fig. 6b).

Preliminary pharmacokinetic analysis indicated that neuroprotective brain levels were not reached following single oral or intraperitoneal administration of indolinone A (50 mg/kg) (data not shown), whereas continuous icv infusion (0.5 nmol/h for 24 h) by osmotic minipumps resulted in brain levels of approximately 0.4 μM.

Continuous icv infusion of the CDK5-inhibiting compound indolinone A, starting 24 h before the insult, significantly reduced infarct volume at 24 h after MCA occlusion (88.5 ± 25.2 mm^3 vs 214.0 ± 43.7 mm^3, mean ± SEM, $n = 5$). Unfortunately, we could not test indolinone D in the MCA occlusion model because of its limited solubility and because only minute amounts of this compound are currently available.

CDK5 contributes to neuronal cell death upstream of mitochondrial dysfunction

Next we asked where CDK5 was positioned within the cell death cascade. In particular, we aimed at determining whether inhibition of CDK5 was sufficient to preserve mitochondrial integrity, a likely prerequisite for long-term

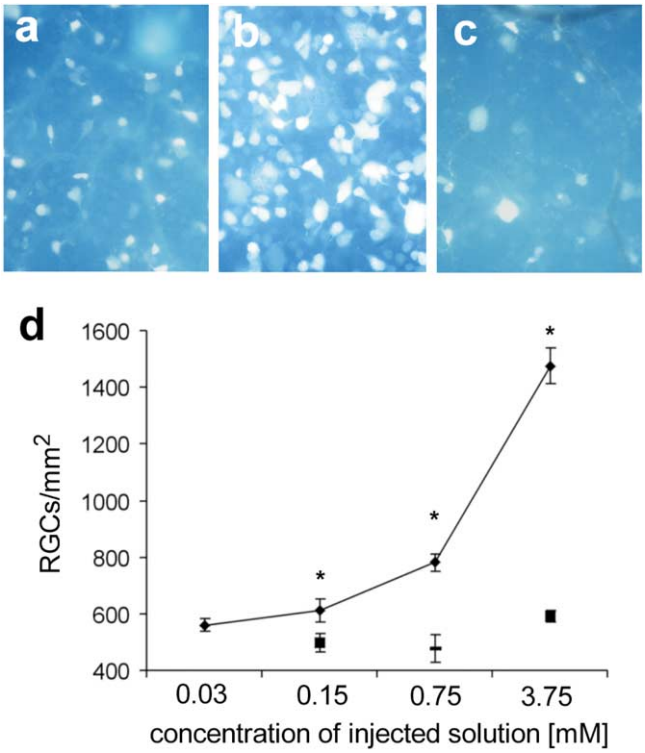

Fig. 5. Inhibition of CDK5 protects axotomized rat retinal ganglion cells in vivo. Retinal whole mounts of retrogradely labeled retinal ganglion cells (RGCs) 14 days after axotomy under treatment with vehicle (a), indolinone A (b), or indolinone B (c). (d) Quantification of surviving RGCs per square millimeter in retinal whole mounts. (◆) Indolinone A treatment. (■) Vehicle controls (two different percentages of DMSO were tested, corresponding to the respective DMSO content of injected indolinone solution). (—) Indolinone B treatment.

rescue of injured neurons. Both indolinone A (Fig. 7a) and indolinone D (data not shown) (1 μM each) prevented staurosporine-induced release of cytochrome c from mitochondria in cultured cortical neurons, suggesting that CDK5 is activated upstream of mitochondrial dysfunction, and CDK5 inhibition has mitochondrio-protective effects. In line with this hypothesis, loss of mitochondrial transmembrane potential in CGNs after BSO treatment, as indicated by JC-1 staining, was also prevented by indolinone A (data not shown) and indolinone D (Figs. 7b–e) (1 μM each). Indolinone B, our cell cycle inhibitor that lacks activity against CDK5, did not prevent the decline in mitochondrial transmembrane potential (up to 1 μM, data not shown), and was not neuroprotective, as already described above.

The caspase inhibitor zVAD-fmk (100 μM) was less neuroprotective than indolinones A and D. It could not prevent the drop in mitochondrial transmembrane potential after BSO treatment as well, while neuronal cell bodies appeared intact (Fig. 7d).

Several protein kinases have been detected within mitochondria (e.g., PDH kinase, PKA, GSK-3β) that modulate mitochondrial electron flow and free radical production (Raha et al., 2002). To exclude an inhibitory effect of our compounds on mitochondria-resident kinases, isolated mitochondria were incubated with indolinones (up to 1 μM) and transmembrane potential was assessed by JC-1 staining. Neither indolinone A nor indolinone D affected basal mitochondrial trans-membrane potential (111.1 $\pm$ 10.2 and 107.9 $\pm$ 13.7% of control value, respectively, mean $\pm$ SD, $n = 4$–5). Treatment of isolated mitochondria with high concentrations of calcium (100 nmol/mg) led to a significant decrease in transmembrane potential (63.7 $\pm$ 5.0% of control value), which was not significantly prevented by co-administration of 1 μM indolinone A or D (72.6 $\pm$ 10.2 and 75.3 $\pm$ 13.7%, respectively, of control value), demonstrating that isolated mitochondria are able to depolarize in the presence of these compounds. These findings indicate that preservation of JC-1 staining in BSO-treated neurons by indolinones A and D is not due to a nonspecific effect on mitochondrial activity.

Discussion

We present four highly potent small molecule kinase inhibitors that we have extensively characterized with respect to their inhibitory effectiveness against CDKs and other kinases that have been associated with neuronal cell death (e.g., JNK, p38 MAPK, ERK1/2). We show that compounds with inhibitory activity against CDK5, but not those blocking the cell cycle-promoting CDK1, -2, or -4, are

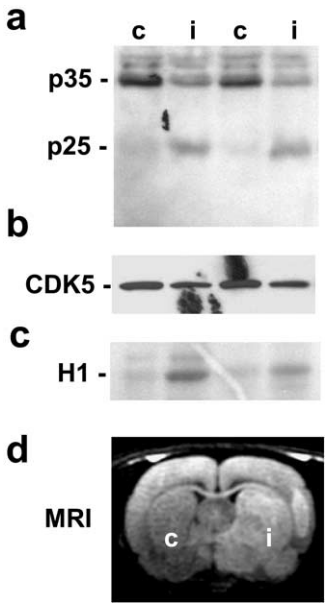

Fig. 6. Cleavage of p35 to p25 and increase in CDK5 activity following focal cerebral ischemia in rats. Occlusion of the medial cerebral artery (MCA) for 2 h and reperfusion for 4 h induce cleavage of p35 to p25 as shown by Western blot analysis (a). While CDK5 (CDK5) expression is slightly decreased (b), histone H1 kinase assay demonstrates a significantly elevated CDK5 activity (c). (d) Diffusion-weighted cerebral magnetic resonance imaging demarcates the ischemic lesion 4 h after reperfusion. i, ischemic hemisphere; c, contralateral hemisphere; H1, histone H1.

neuroprotective in several in vitro and in vivo paradigms. Furthermore, we delineate the position of CDK5 within the cell death cascade upstream of mitochondrial dysfunction.

Pan-CDK inhibitors, such as olomoucine, roscovitine, and flavopiridol, proved to be neuroprotective before. For instance, these compounds have been used to treat trophic factor-deprived PC12 cells and differentiated sympathetic neurons or cultured embryonic cortical neurons exposed to DNA-damaging agents. Most recently, neuroprotection by flavopiridol was demonstrated following focal cerebral ischemia in rats (Park et al., 1996, 1997a, b, 1998; Padmanabhan et al., 1999; Osuga et al., 2000; Konishi et al., 2002). These results provide functional support for the hypothesis that pro-apoptotic stimuli induce an abortive, and eventually fatal, cell cycle reentry in postmitotic neurons (Heintz, 1993). Besides pharmacological CDK inhibitors, negative mutants of CDK4/6, and cdc2 (= CDK1) also protected neurons from death (Park et al., 1997a, b; Konishi et al., 2002), and upregulation of cell cycle molecules, such as cyclin D1, E2F1, and CDK4, has been reported in the context of neuronal apoptosis (Freeman et al., 1994; Park et al., 1996; Padmanabhan et al., 1999).

These results, however, still left open the possibility that CDK5, which is not involved in cell cycle control, also contributes to neuronal cell death. For example, it turns out that all of the neuroprotective small molecule CDK inhibitors, like olomoucine and flavopiridol, strongly inhibit CDK5 as well as other members of the CDK family (Leclerc et al., 2001). Thus, the effectiveness of so-called cell cycle inhibitors against neuronal apoptosis is in accordance with the possibility that CDK5 is an important upstream cell death promoter, at least in some neuronal cell death paradigms. Moreover, the exact specificity of dominant-negative CDK mutants within the CDK family has not been published, and they may also cross-inhibit CDK5 by competing with common substrates or modulating upstream binding partners.

In the neuronal cell death models that we used, inhibitory activity against CDK5, but not cell cycle-relevant CDKs, was associated with neuroprotective properties. Indolinones B and C, which have IC_{50} values with respect to CDK1, -2, and -4 in the low nanomolar to subnanomolar range and effectively inhibit proliferation of tumor cells, did not display any neuroprotective properties. This makes a significant contribution by cell cycle CDKs in the models that we investigated very unlikely. Moreover, the neuroprotective potency of indolinone D, which lacks cell cycle-inhibiting properties at the highest concentration tested, further supports the notion that CDK5 inhibition was necessary, and sufficient, for neuroprotection in our experiments. The data obtained with indolinone D are also the first pharmacological proof that CDK5 is dispensable for cell cycle progression.

Our data do not necessarily conflict with published evidence supporting an important role of cell cycle elements for neuronal apoptosis in many paradigms. We cannot exclude an additional contribution of cell cycle functions other than activity of mitotic CDKs to neuronal cell death, even in the paradigms used in this study. Moreover, the fact that blocking cell cycle-relevant CDKs was not neuroprotective in our study does not exclude that other molecules that can be involved in cell cycle regulation, like retinoblastoma protein and E2F, can modulate neuronal cell death by influencing pathways unrelated to cell cycle progression. We suppose that the role of CDK5, and other CDKs, may strongly depend on the experimental paradigm or developmental stage of the neuronal cells examined. For example, immature cerebellar granule neurons (DIV 2) have been used for the in vitro study demonstrating neuroprotection by a dominant-negative cdc2 mutant (Konishi et al., 2002). Here, the role of CDK family members might be different compared with the situation in the more mature neurons, e.g., CGNs at DIV 7, that have been used in our study and that do not express cdc2 (Courtney and Coffey, 1999).

A general caveat has to be expressed regarding the specificity of small molecule kinase inhibitors. Since 518 putative protein kinase genes have been identified in the human genome (Manning et al., 2002), it is impossible to exclude any cross-inhibition of other, even unknown, kinases. However, we have extensively analyzed indolinones A–D with respect to their inhibitory effectiveness against CDKs and other kinases that have been associated with neuronal cell death. In addition, the fact that inhibitory activity against CDK5 clearly correlated with neuroprotection across four compounds makes a confounding effect even more unlikely.

Moreover, previous studies support the hypothesis that CDK5 is an important player during neuronal cell death. CDK5 has been co-localized with Lewy bodies (Nakamura et al., 1997), a hallmark of Parkinson's disease. Furthermore, abnormal accumulation of p25 and overactivation of CDK5 were observed in a transgenic mouse model for ALS (Nguyen et al., 2001), cultured cortical neurons exposed to amyloid-β (Lee et al., 2000), and brains from patients with Alzheimer's disease (Patrick et al., 1999), supporting a role for CDK5 in neuronal cell death in neurodegenerative diseases. With respect to amyloid-β-mediated neuronal toxicity, overactivation of CDK5 is caused by proteolytic conversion of the CDK5 activator p35 to p25 by calpain, a calcium-activated protease. p25 leads to pathologically increased activity and subcellular redistribution of CDK5 (Lee et al., 2000). We were able to confirm this mechanism in vivo following transient focal cerebral ischemia in rats, demonstrating cleavage of p35 to p25 with a subsequent increase in CDK5 activity. However, in all other paradigms examined, we did not find p35 cleavage or upregulation of p35 or its homologue, p39. This is in accordance with a recent study describing a free radical-induced increase in CDK5 activity, although CDK5 and p35 protein levels remain unchanged (Gong et al., 2003). Few other mechanisms that result in increased CDK5 activity have been identified to date. It has been shown that CDK5 becomes phosphorylated at tyrosine 15 by c-Abelson kinase, which increases

CDK5 kinase activity. (Zukerberg et al., 2000). Using a phospho-specific antibody (Santa Cruz) for Western blot analysis, however, we were unable to detect a specific band at 32 kDa (data not shown). Overall, while we present evidence supporting the general importance of CDK5 for neuronal cell death, the upstream events leading to CDK5 overactivation seem to vary between experimental paradigms and involve p35/p25-dependent as well as -independent mechanisms. Moreover, whether CDK5 needs to be overactivated to instigate the death cascade or blocking physiological CDK5 activity is sufficient to halt cell demise remains to be shown.

We demonstrate that CDK5 inhibition prevents a drop in mitochondrial transmembrane potential and release of mitochondrial cytochrome c following BSO and staurosporine treatment, respectively. This is in line with our finding that an inhibitor of caspases, which acts predominantly downstream of mitochondrial dysfunction, was less effective and, in our hands, did not protect neurons from a decline in mitochondrial transmembrane potential. Our compounds did not prevent the decline in transmembrane potential in isolated mitochondria following calcium overload. This suggests that CDK5 or its substrate translocates to mitochondria during neuronal cell death, similar to cell cycle CDKs, which phosphorylate mitochondrial Bcl-2 family members in proliferating cells in vitro (Vantieghem et al., 2002). However, as the molecular link between CDK5 and mitochondria is not clear yet, the mechanism by which deregulated CDK5 activity results in mitochondrial dysfunction might even be more indirect, possibly involving changes in gene transcription. For example, in a very recent study it was shown that CDK5-dependent phosphorylation abolishes the neuroprotective effects of the transcription factor MEF2 (Gong et al., 2003).

The mitochondria-protective effect of CDK5 inhibition may explain our observation that blocking CDK5 was effective in various neuronal cell death models, ranging from apoptotic-like death (growth factor withdrawal of RGCs, CGNs after staurosporine treatment or potassium/serum deprivation) to paradigms with prevalent features of necrosis (CGNs exposed to BSO, focal cerebral ischemia in rats). It has been proposed that the mode of cell death is determined by the cellular energy state, which depends on mitochondrial integrity (Ankarcrona et al., 1995; Nicotera et al., 1998). According to this hypothesis, the decision whether a cell dies by necrosis or an energy-requiring apoptotic process is made at the level of mitochondria. Consistently, our CDK5 inhibitor prevented mitochondrial dysfunction and early necrosis in the BSO paradigm. Surviving neurons, however, displayed delayed apoptotic DNA cleavage, indicating a shift from necrosis to apoptosis during sustained glutathione depletion.

Taken together, our data do not exclude pro-apoptotic consequences of an incomplete cell cycle reactivation or specific elements of the cell cycle machinery as previously described. However, in our apoptotic- and necrotic-like neuronal cell death paradigms, CDK5, but not cell cycle CDKs, is an important death-promoting factor. Moreover, we delineate the position of CDK5 within the cell death cascade. Due to its early action in the death process, CDK5 might turn out to be a suitable target of functional long-term rescue of neurons in the context of neurodegenerative diseases. CDK5 activity is restricted to neurons and dispensable for cell cycle progression. Therefore, selective CDK5 inhibitors will not affect proliferating cells, e.g., of the immune system or the intestine, and may turn out to be of great value in the treatment of neurodegenerative diseases. Finally, our findings underline the general importance of mitochondrio-protective strategies for therapeutic approaches aiming at the prevention of neuronal cell death.

Experimental methods

Optic nerve transection in the rat

Optic nerve transection of adult female Sprague–Dawley rats (200–250 g; Charles River Wiga, Sulzfeld, Germany; $n = 4$ or 5 per group), retrograde labeling, tissue processing, and cell counting were done as described previously (Klöcker et al., 1998; Kermer et al., 2001). For drug administration, CDK inhibitors were dissolved in dimethyl sulfoxide (DMSO; Sigma, Germany) and diluted for intravitreal administration in ddH_2O/DMSO. Appropriate vehicle controls for 2 and 15% DMSO in ddH_2O did not result in enhanced survival of RGCs (see Results). Intraocular injection (2 μl) of inhibitors or vehicle on Days 0, 4, 7, and 10 postlesion was performed as described (Klöcker et al., 1998; Kermer et al., 2001).

Focal cerebral ischemia

Male Sprague–Dawley rats (280–300 g) were anesthetized with 2% halothane in air. Body temperature was monitored with a rectal probe and maintained at 37°C during ischemia. The right common carotid artery and the right external carotid artery were exposed and ligated. Approximately 16–19 mm of 4-O silicone-coated nylon suture was threaded into the internal carotid artery through the common carotid artery up to the anterior cerebral artery to block the origin of the middle cerebral artery (MCA). After 2 h, animals were reanesthetized and the nylon suture was retracted to allow reperfusion. Ischemia/reperfusion was confirmed by laser Doppler (Perimed) measurements of cortical blood flow. Ischemic brain areas were visualized by perfusion- and diffusion-weighted magnetic resonance imaging using a 4.7-T BIOSPEC 47/40 system (Bruker), and were subsequently dissected for biochemical analysis. Infarct size was evaluated by triphenyltetrazolium chloride (TTC) staining of brain slices and computer-assisted densitometric analysis. For drug administration, compound (0.5 mM in

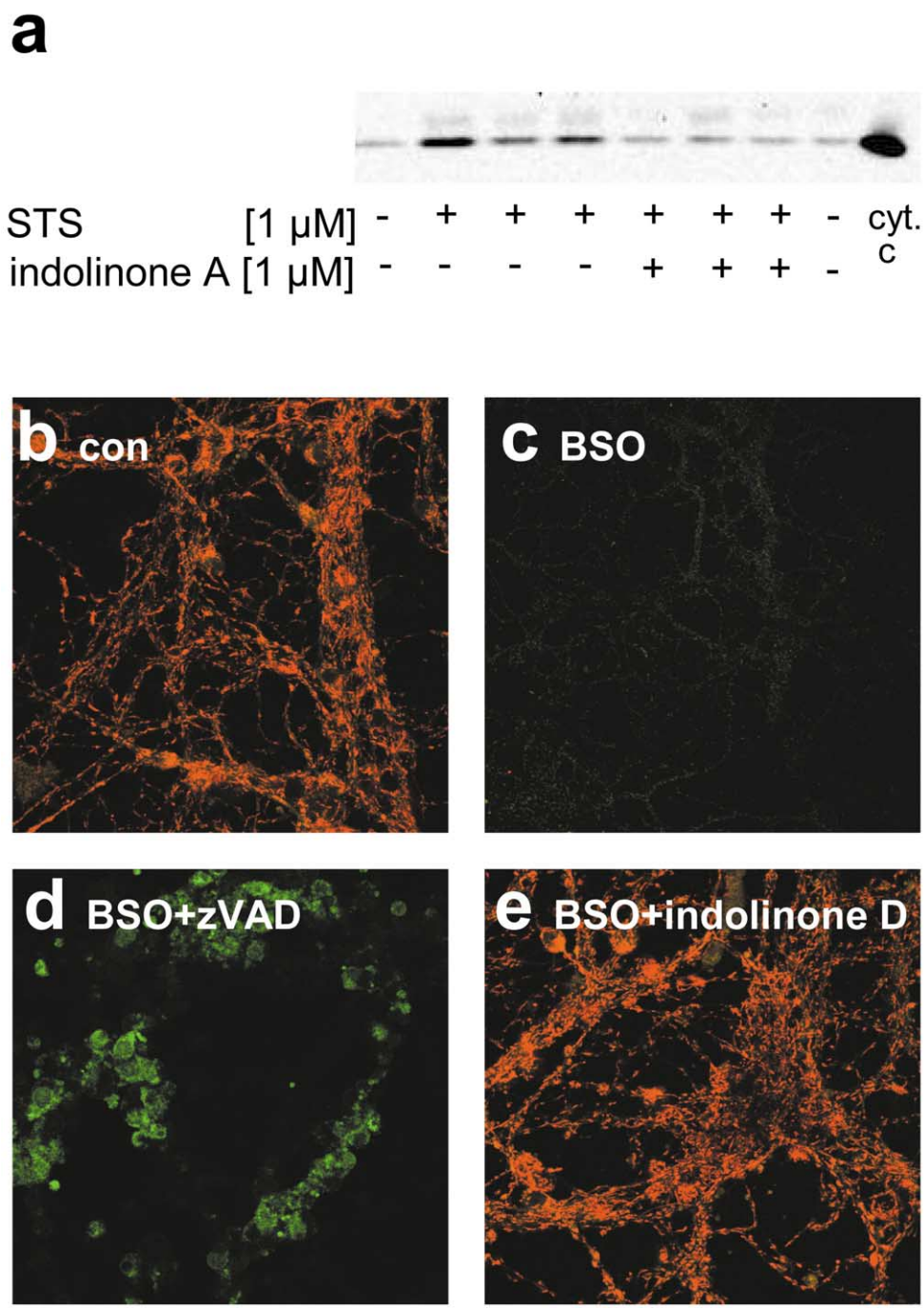

Fig. 7. CDK5 inhibition prevents mitochondrial cytochrome c release and loss of mitochondrial transmembrane potential. (a) CDK5 inhibition by indolinone A (1 μM) inhibits staurosporine-induced mitochondrial cytochrome c release in rat cortical neurons. Western blot analysis showing cytosolic cytochrome c levels in control cultures, after staurosporine treatment and co-treatment with staurosporine and indolinone A. cyt. c, recombinant cytochrome c as positive control. (b–e) Indolinone *D* (1 μM) prevents loss of mitochondrial transmembrane potential induced by 36 h BSO treatment of CGNs. JC-1 shows a potential-dependent accumulation in mitochondria and a concentration-dependent formation of J aggregates, leading to a reversible shift in fluorescence emission from green to red in hyperpolarized mitochondria. (b) Control CGN culture showing red JC-1 signal, indicative of hyperpolarized mitochondria. (c) Free radical stress induced by BSO treatment induces loss of mitochondrial transmembrane potential and subsequent cell death (only cell debris remains visible). (d) Caspase inhibition by zVAD-fmk prevents BSO-induced cell loss, but fluorescence emission shift from red to green indicates depolarization of mitochondria. (e) Indolinone D treatment prevents neuronal cell death and preserves mitochondrial transmembrane potential.

sterile H_2O) or vehicle solution was poured into osmotic minipumps (Alzet 1003D). A cannula (Alzet brain infusion kit) was stereotactically introduced into the right lateral ventricle and connected to the minipump placed subcutaneously in the neck. Solutions were infused at the rate of 1 μl/h starting 24 h before ischemia (Osuga et al., 2000).

Western blot analysis

Western blot experiments to determine the expression of p35, p39, and CDK5 in rat tissue and cultured neurons were performed as described earlier (Klöcker et al., 1998; Kermer et al., 2001). Primary antibodies were rabbit polyclonal antibodies directed against p35 (C-19, Santa Cruz Biotechnology, Santa Cruz, CA, USA); p39 (affinity purified on p39-GST, a kind gift of L.-H. Tsai, Harvard Medical School, Boston, MA, USA); cytochrome c (BD Pharmingen, Heidelberg, Germany); and CDK5 (C-8, Santa Cruz Biotechnology).

Immunohistochemistry

Immunohistochemical experiments using rat retinas were performed as described before (Klöcker et al., 1998; Kermer et al., 2001). Briefly, rats received an overdose of chloral hydrate and were perfused intracardially with 4% paraformaldehyde in PBS for 10 min. Then, both eyes were dissected and immersion-fixed as eye cups without cornea and lens for an additional 20 min in 4% paraformaldehyde in PBS at 4°C. Eye cups were immersed in 30% sucrose in PBS at 4°C overnight and snap-frozen in liquid nitrogen. Sixteen-micrometer cryostat sections were collected on gelatin-coated slides, air-dried, and stored at −20°C before processing. Retinal sections were preincubated in 10% normal goat serum in PBS containing 0.3% Triton X-100 for 1 h at room temperature. Sections were then washed three times in PBS and incubated with the primary antibody at 4°C overnight. Omission of the primary antibody served as negative control. Immunoreactivity was visualized by incubating the sections with a secondary fluorescence antibody (1:200, see below) after washing three times with PBS. Finally, sections were coverslipped in Mowiol (Hoechst, Fankfurt, Germany). At least three different animals per experimental group were examined.

Primary antibody was a rabbit polyclonal antibody directed against p39 (see above). FITC-conjugated goat anti-rabbit IgG was used as secondary antibody (Dianova, Hamburg, Germany).

Cell culture

For immunopurified rat RGC culture, rat pups were sacrificed on Postnatal Day 8. RGCs were purified according to a two-step panning protocol described previously (Barres et al., 1988). As culture medium, we used serum-free neurobasal medium (Gibco, Eggenstein, Germany), supplemented with glutamine, cysteine, pyruvate, triiodothyronine, B-27 supplement, and Sato (BSA, transferrin, progesterone, putrescine, sodium selenite). During the first 24 h, RGCs were additionally incubated with saturating concentrations of forskolin, human BDNF, CNTF, and insulin. RGCs were withdrawn from neurotrophins by changing the medium on Culture Day 1 and incubated with the respective compounds.

CGNs were isolated from 7-day-old Wistar rat pups and were purified by density sedimentation. Briefly, cerebella were removed and dissociated with 1% trypsin/0.05% DNase in calcium- and magnesium-free Hanks' balanced salt solution ($HBSS^-$; Gibco) for 13 min at room temperature. After two washing steps with $HBSS^-$ to dilute trypsin, 0.5% DNase in $HBSS^-$ was added and the cerebella were dissociated by trituration using Pasteur pipets. CGNs were subsequently separated by centrifugation at 1300*g* for 15 min in a 40% (v/v) Percoll solution. The cells were harvested from the pellet and washed in ice-cold basal modified Eagle's medium, supplemented with 2 mM glutamine (BME, Gibco) followed by centrifugation for 5 min at 150*g*. Thereafter, 90,000 viable cells per well were plated on poly-L-lysine-coated (Becton Dickinson) 96-well plates, in BME supplemented with 10% heat-inactivated fetal bovine serum, 25 mM KCl, 100 U/ml penicillin, and 100 μg/ml streptomycin (Biochrom). After 24 h in culture, the cells were treated with cytosine arabinoside (Sigma) at a final concentration of 5 μM. Cultures were maintained at 37°C, 5% CO_2 for 7 days without a change in medium. At DIV 7, cells were washed once and subsequently incubated in BME containing 5 mM KCl (potassium/serum deprivation). Alternatively, culture medium was changed to BME plus 25 mM KCl and CGNs were treated with staurosporine (1 μM; Sigma, St. Louis, MO, USA), or the glutamylcysteine synthetase inhibitor L-buthionine sulfoximine (0.5 mM) (Wüllner et al., 1999). Compounds were tested at DIV 7, when expression of CDK1, -2, and -4 in CGNs is downregulated, whereas CDK5 is upregulated (Courtney and Coffey, 1999).

Cortical neurons were isolated from E15 rat embryos as described previously (Muller et al., 1984). Cells were seeded in serum-free neurobasal medium (Gibco) supplemented with B27 additive and 0.5 mM L-glutamine. Culture medium was replaced with fresh neurobasal medium every 72 h. Experiments were performed after 7 days in vitro (DIV 7).

SKUT-1B uterine tumor cells were cultured as described by Bamberger et al., (1997).

Assessment of cell viability

Mitochondrial metabolic activity was tested using either the MTT assay (Barres et al., 1988) or the Alamar blue Assay (Serotec, Oxford, UK). These assays use an indicator compound that changes from the oxidized, non fluorescent to the reduced, fluorescent form in response to chemical reduction resulting from cellular metabolic activity.

MTT (5 mg/ml) was added to culture wells (1:10) and incubated at 37°C for 1 h. Viability of RGCs was assessed by counting six fields within a culture well at a magnification of 200×. RGCs showing dense blue staining of cell bodies were considered MTT-positive. Survival of RGCs

under the different culture conditions was calculated as a percentage of mean values of MTT-positive RGCs/mm^2 in two wells for Day 3 and Day 1.

Alamar blue solution was added to the medium at a final concentration of 5%. CGNs were incubated for 2 h; thereafter fluorescence was monitored at 530nm excitation and 590nm emission wavelengths in a Millipore CytoFluor Reader 2350.

Mitochondrial membrane potential was assessed using the cationic dye JC-1 (Molecular Probes). JC-1 shows a potential-dependent accumulation in mitochondria and a concentration-dependent formation of J aggregates leading to a reversible shift in fluorescence emission from green to red in hyperpolarized mitochondria. CGNs cultured on Lab-Tek Chambered Coverglass were incubated with JC-1 solution (3 μM in sterile, tissue culture-grade PBS) for 30 min. After three washing steps in PBS confocal laser scan microscope images (Leica TCS) were acquired at 488nm excitation wavelength and dual emission at 530 $\pm$ 15- and $\geq$590-nm wavelengths.

Cell viability was also assayed using the LIVE/DEAD Viability/Cytotoxicity Kit (Molecular Probes). CGNs cultured on Lab-Tek Chambered Coverglass were incubated with calcein acetoxymethyl ester (calcein AM, 4 μM in sterile, tissue culture-grade PBS) and ethidium homodimer (EthD-1, 2 μM) for 30 min. In viable cells, the nonfluorescent, cell-permeant calcein AM is hydrolyzed by intracellular esterases, yielding the green fluorescent, polyanionic calcein. EthD-1 enters only necrotic cells with damaged plasma membranes. Its red fluorescence increases by 40-fold after binding to nucleic acids. Confocal laser scan microscope images (Leica TCS) were acquired at 488nm excitation wavelength and dual emission at 515 $\pm$ 15- and $\geq$620nm wavelengths.

Apoptotic DNA fragmentation was measured with a quantitative sandwich immunoassay using biotinylated anti-histone antibodies and peroxidase-conjugated anti-DNA antibodies as described in the manufacturer's protocol (Cell Death Detection ELISA, Roche, Mannheim, Germany).

Formation of intracellular reactive oxygen species following glutathione depletion was detected by loading the cells with the fluorescent indicator dichlorodihydrofluorescein diacetate (DCFDA, Molecular Probes; final concentration 100 μM) for 1 h. After washing in phenol red-free BME, fluorescence intensity was assessed using either a Millipore CytoFluor Reader 2350 or a LEICA TCS confocal laser scan microscope at 488-nm excitation and 525-nm emission wavelengths. As a positive control, H_2O_2 (final concentration 200 μM) was added to control cultures.

Isolation of mitochondria

C57/BL6 mice (20–25 g) were used for the isolation of forebrain mitochondria as described earlier (Sims; 1990) with modifications. Animals were fasted overnight and killed by decaptation. All steps were performed at 4°C. Forebrains were rapidly dissected and collected in isolation buffer (210 mM mannitol, 70 mM sucrose, 1 mM EDTA, 5 mM Hepes, pH 7.4). After extensive washing, forebrains were homogenized in 10% (w/v) isolation buffer using a Teflon in-glass potter homogenizer. The homogenate was centrifuged for 4 min at 1400*g*. The supernatant was separated and the pellet was homogenized and centrifuged again as described above. Both supernatants were pooled and subsequently centrifuged for 5 min at 30,700*g*. The pellet (containing myelin, synaptosomes, and mitochondria) was resuspended in 15% (v/v) Percoll in HES buffer (5 mM Hepes, 1 mM EDTA, 0.32 M sucrose, pH 7.4) and layered on top of a discontinuous 25–40% (v/v) Percoll gradient in HES buffer. After centrifugation for 5 min at 30,700*g* the interphase fraction was diluted 1:4 with EDTA-free isolation buffer and centrifuged 10 min at 16,700*g*. The pellet was washed in EDTA-free isolation buffer and centrifuged 10 min at 7300*g*. The resulting pellet was resuspended in EDTA-free isolation buffer (about 20 mg of protein/ml). The respiratory control ratio, an indicator of the metabolic integrity of the mitochondria, was higher than 4, when malate (2.5 mM) and pyruvate (5 mM) were used as substrates. All subsequent experiments were performed within 3 h of isolation.

The assay (0.5 mg/ml) was performed in 100 μl incubation buffer (5 mM Tris–HCl, 100 mM KCl, 70 mM mannitol, 30 mM sucrose, 1 mM $MgCl_2$, pH 7.4), containing malate and pyruvate as respiratory substrates and the potential-sensitive fluorescent dye JC-1 (2.5 μM; Molecular Probes). Mitochondrial membrane potential was measured in a microtiter plate reader (Fluoroskan Ascent, Labsystems) in the dual-wavelength kinetic mode at excitation wavelength 487-nm and emission wavelengths at 530 nm followed by 590 nm. Isolated mice forebrain mitochondria were preincubated in compound or vehicle at room temperature for 10 min. Thereafter, calcium (100 nmol/mg), FCCP (1 μM), or vehicle was added to the mitochondria, and JC-1 fluorescence was measured each minute. Mitochondrial membrane potential is expressed as the ratio of the relative fluorescence units obtained at 590 and 530 nm.

Kinase preparations and assays used to analyze inhibition of CDKs by indolinones

Human recombinant p25 was expressed in *Escherichia coli* as glutathione *S*-transferase fusion protein and purified by glutathione affinity chromatography. His-Cdk5 was obtained from baculovirus-infected Hi5 insect cells (vectors kindly provided by L-H Tsai) (Nikolic et al., 1998). GST-p25/Cdk5-His was reconstituted by mixing equal amounts of recombinant human proteins, and was purified by NTA-agarose chromatography.

Cyclin-dependent kinase activity (Cdk1/CyclinB1, Cdk2/CyclinE, Cdk4/CyclinD1, Cdk5/p25) was assessed as has recently been described (Davies et al., 2000; Evans et al., 2002) with minor modifications. Briefly, a 96-well filter

plate assay (MultiScreen, Millipore, Eschborn, Germany) was performed in assay buffer (25 mM Mops, 4 mM $MgCl_2$, 1 mM DTT, pH 7.0) containing 5 μg histone H1, 7.5 μM cold ATP, and 1 μCi [γ-^{33}P]ATP. Alternatively, 1 μM biotinylated peptide (biotin-PKTPKKAKKL) derived from the Cdk5 phosphorylation site of histone H1 was used as substrate in a scintillation proximity assay (Amersham Bioscience, Uppsala, Sweden). Following incubation at room temperature for 40 min, streptavidin-coated polystyrene beads were added and incorporated radioactivity was monitored in a liquid scintillation counter.

Immunoprecipitation and kinase assay for quantification of CDK5 activity in neuronal protein lysates

CDK5 immunoprecipitation and kinase assay were performed as originally described by Tsai et al. (1993) with modifications. Briefly, brain hemispheres or cerebellar granule neurons (2.5×10^7) were Dounce-homogenized in lysis buffer containing 50 mM Tris–HCl, pH 7.5, 150 mM NaCl, 5 mM EDTA, 1% Triton X-100, 1 mM DTT, 10 mM sodium fluoride, 1 mM glycerophosphate, 1 mM sodium orthovanadate, 2.5 mM disodium pyrophosphate, 1 mM aminoethyl-benzolsulfonylfluoride, and protease inhibitor cocktail (Complete, EDTA-free, Roche, Mannheim). Homogenates were centrifuged at 12,000*g* for 15 min. Three hundred micrograms (CGNs) or 1.0 mg (brain hemispheres) total cellular protein was used for immunoprecipitation with anti-Cdk5 antibody (10 μg, C-8, Santa Cruz, Heidelberg, Germany) and protein A–Sepharose beads. Antibody was omitted as negative control. Immunoprecipitates were rinsed three times with lysis buffer and three times with kinase buffer (50 mM Tris–HCl, pH 7.5, 4 mM $MgCl_2$, 5 mM $MnCl_2$, 1 mM DTT, 2.5 mM EGTA, 1 mM sodium fluoride, 10 mM glycerophosphate, 0.1 mM sodium orthovanadate, 2.5 mM disodium pyrophosphate, 15 mM nitrophenyl phosphate, and 1 μM cold ATP). The washed beads were incubated with kinase buffer containing 10 μg histone H1 and 10 μCi of [γ-^{32}P]ATP in a final volume of 25 μl at 30°C for 30 min. Thereafter, 10 μl of 5× Laemmli sample buffer was added to each sample. After boiling for 5 min samples were analyzed by SDS–PAGE and autoradiography. Bands were densitometrically evaluated using a Bio-Rad MultiImager and Quantity One software (Bio-Rad, Munich, Germany).

Other laboratory chemicals were obtained from Sigma.

Statistics

Data are given as means ± SEM unless otherwise stated. Statistical significance was assessed with a one-way ANOVA followed by Duncan's post hoc test. An asterisk indicates significance at $P \leq 0.05$.

Acknowledgments

We thank Professor P. Cohen and Dr. N. Redemann for help with kinase activity assays, Dr. L.-H. Tsai for providing p39 antibody, and C. Bentz, H. Eberhardt, and B. Kramer for excellent technical assistance.

References

Ankarcrona, M., Dypbukt, J.M., Bonfoco, E., Zhivotovsky, B., Orrenius, S., Lipton, S. A., Nicotera, P., 1995. Glutamate-induced neuronal death: a succession of necrosis or apoptosis depending on mitochondrial function. Neuron 15, 961–973.

Bamberger, A.M., Jenatschke, S., Erdmann, I., Schulte, H.M., 1997. Progestin-dependent stimulation of the human leukemia inhibitory factor promoter in SKUT-1B uterine tumor cells. J. Reprod. Immunol. 33, 189–201.

Barres, B.A., Silverstein, B.E., Corey, D.P., Chun, L.L., 1988. Immunological, morphological, and electrophysiological variation among retinal ganglion cells purified by panning. Neuron 1, 791–803.

Chae, T., Kwon, Y.T., Bronson, R., Dikkes, P., Li, E., Tsai, L.H., 1997. Mice lacking p35, a neuronal specific activator of Cdk5, display cortical lamination defects, seizures, and adult lethality. Neuron 18, 29–42.

Copani, A., Condorelli, F., Caruso, A., Vancheri, C., Sala, A., Giuffrida Stella, A.M., Canonico, P.L., Nicoletti, F., Sortino, M.A., 1999. Mitotic signaling by beta-amyloid causes neuronal death. FASEB J. 13, 2225–2234.

Courtney, M.J., Coffey, E.T., 1999. The mechanism of Ara-C-induced apoptosis of differentiating cerebellar granule neurons. Eur. J. Neurosci. 11, 1073–1084.

Davies, S.P., Reddy, H., Caivano, M., Cohen, P., 2000. Specificity and mechanism of action of some commonly used protein kinase inhibitors. Biochem. J. 351, 95–105.

Evans, D.B., Rank, K.B., Sharma, S.K., 2002. A scintillation proximity assay for studying inhibitors of human tau protein kinase II/cdk5 using a 96-well format. J. Biochem. Biophys. Methods 50, 151–161.

Floyd, S.R., Porro, E.B., Slepnev, V.I., Ochoa, G.C., Tsai, L.H., De Camilli, P., 2001. Amphiphysin 1 binds the cyclin-dependent kinase (cdk) 5 regulatory subunit p35 and is phosphorylated by cdk5 and cdc2. J. Biol. Chem. 276, 8104–8110.

Freeman, R.S., Estus, S., Johnson Jr., E.M., 1994. Analysis of cell cycle-related gene expression in postmitotic neurons: selective induction of cyclin D1 during programmed cell death. Neuron 12, 343–355.

Gong, X., Tang, X., Wiedmann, M., Wang, X., Peng, J., Zheng, D., Blair, L.A., Marshall, J., Mao, Z., 2003. CDK5-mediated inhibition of transcription factor MEF2 in neurotoxicity-induced apoptosis. Neuron 38, 33–46.

Heintz, N., 1993. Cell death and the cell cycle: a relationship between transformation and neurodegeneration? Trends Biochem. Sci. 18, 157–159.

Hirooka, K., Tomizawa, K., Matsui, H., Tokuda, M., Itano, T., Hasegawa, E., Wang, J.H., Hatase, O., 1996. Developmental alteration of the expression and kinase activity of cyclin-dependent kinase 5 (Cdk5)/p35nck5a in the rat retina. J. Neurochem. 67, 2478–2483.

Kermer, P., Klöcker, N., Bähr, M., 1999. Neuronal death after brain injury: models, mechanisms, and therapeutic strategies in vivo. Cell Tissue Res. 298, 383–395.

Kermer, P., Klöcker, N., Weishaupt, J.H., Bähr, M., 2001. Transection of the optic nerve in rats: Studying neuronal death and survival in vivo. Brain Res. Brain Res. Protocis. 7, 255–260.

Klöcker, N., Cellerino, A., Bähr, M., 1998. Free radical scavenging and inhibition of nitric oxide synthase potentiates the neurotrophic effects

of brain-derived neurotrophic factor on axotomized retinal ganglion cells in vivo. J. Neurosci. 18, 1038–1046.

Konishi, Y., Lehtinen, M., Donovan, N., Bonni, A., 2002. Cdc2 phosphorylation of BAD links the cell cycle to the cell death machinery. Mol. Cell. 9, 1005–1016.

Leclerc, S., Garnier, M., Hoessel, R., Marko, D., Bibb, J.A., Snyder, G.L., Greengard, P., Biernat, J., Wu, Y.Z., Mandelkow, E.M., Eisenbrand, G., Meijer, L., 2001. Indirubins inhibit glycogen synthase kinase-3 beta and CDK5/p25, two protein kinases involved in abnormal tau phosphorylation in Alzheimer's disease: a property common to most cyclin-dependent kinase inhibitors? J. Biol. Chem. 276, 251–260.

Lee, M.S., Kwon, Y.T., Li, M., Peng, J., Friedlander, R.M., Tsai, L.H., 2000. Neurotoxicity induces cleavage of p35 to p25 by calpain. Nature 405, 360–364.

Manning, G., Whyte, D.B., Martinez, R., Hunter, T., Sudarsanam, S., 2002. The protein kinase complement of the human genome. Science 298, 1912–1934.

Meyerson, M., Enders, G.H., Wu, C.L., Su, L.K., Gorka, C., Nelson, C., Harlow, E., Tsai, L.H., 1992. A family of human cdc2-related protein kinases. EMBO J. 11, 2909–2917.

Muller, H.W., Beckh, S., Seifert, W., 1984. Neurotrophic factor for central neurons. Proc. Natl. Acad. Sci. USA 81, 1248–1252.

Nakamura, S., Kawamoto, Y., Nakano, S., Ikemoto, A., Akiguchi, I., Kimura, J., 1997. Cyclin-dependent kinase 5 in Lewy body-like inclusions in anterior horn cells of a patient with sporadic amyotrophic lateral sclerosis. Neurology 48, 267–270.

Nguyen, M.D., Lariviere, R.C., Julien, J.P., 2001. Deregulation of Cdk5 in a mouse model of ALS: toxicity alleviated by perikaryal neurofilament inclusions. Neuron 30, 135–147.

Nicotera, P., Leist, M., Ferrando-May, E., 1998. Intracellular ATP, a switch in the decision between apoptosis and necrosis. Toxicol. Lett. 103, 139–142.

Nikolic, M., Chou, M.M., Lu, W., Mayer, B.J., Tsai, L.H., 1998. The p35/Cdk5 kinase is a neuron-specific Rac effector that inhibits Pak1 activity. Nature 395, 194–198.

Nikolic, M., Dudek, H., Kwon, Y.T., Ramos, Y.F., Tsai, L.H., 1996. The cdk5/p35 kinase is essential for neurite outgrowth during neuronal differentiation. Genes Dev. 10, 816–825.

O'Hare, M., Wang, F., Park, D.S., 2002. Cyclin-dependent kinases as potential targets to improve stroke outcome. Pharmacol. Ther. 93, 135–143.

Osuga, H., Osuga, S., Wang, F., Fetni, R., Hogan, M.J., Slack, R.S., Hakim, A.M., Ikeda, J.E., Park, D.S., 2000. Cyclin-dependent kinases as a therapeutic target for stroke. Proc. Natl. Acad. Sci. USA 97, 10254–10259.

Padmanabhan, J., Park, D.S., Greene, L.A., Shelanski, M.L., 1999. Role of cell cycle regulatory proteins in cerebellar granule neuron apoptosis. J. Neurosci. 19, 8747–8756.

Paglini, G., Pigino, G., Kunda, P., Morfini, G., Maccioni, R., Quiroga, S., Ferreira, A., Caceres, A., 1998. Evidence for the participation of the neuron-specific CDK5 activator p35 during laminin-enhanced axonal growth. J. Neurosci. 18, 9858–9869.

Park, D.S., Farinelli, S.E., Greene, L.A., 1996. Inhibitors of cyclin-dependent kinases promote survival of post-mitotic neuronally differentiated PC12 cells and sympathetic neurons. J. Biol. Chem. 271, 8161–8169.

Park, D.S., Levine, B., Ferrari, G., Greene, L.A., 1997a. Cyclin dependent kinase inhibitors and dominant negative cyclin dependent kinase 4 and 6 promote survival of NGF-deprived sympathetic neurons. J. Neurosci. 17, 8975–8983.

Park, D.S., Morris, E.J., Greene, L.A., Geller, H.M., 1997b. G1/S cell cycle blockers and inhibitors of cyclin-dependent kinases suppress camptothecin-induced neuronal apoptosis. J. Neurosci. 17, 1256–1270.

Park, D.S., Morris, E.J., Stefanis, L., Troy, C.M., Shelanski, M.L., Geller, H.M., Greene, L.A., 1998. Multiple pathways of neuronal death induced by DNA-damaging agents, NGF deprivation, and oxidative stress. J. Neurosci. 18, 830–840.

Patrick, G.N., Zukerberg, L., Nikolic, M., de la Monte, S., Dikkes, P., Tsai, L.H., 1999. Conversion of p35 to p25 deregulates Cdk5 activity and promotes neurodegeneration. Nature 402, 615–622.

Raha, S., Myint, A.T., Johnstone, L., Robinson, B.H., 2002. Control of oxygen free radical formation from mitochondrial complex I: roles for protein kinase A and pyruvate dehydrogenase kinase. Free Radical Biol. Med. 32, 421–430.

Reed, J.C., 2000. Mechanisms of apoptosis. Am. J. Pathol. 157, 1415–1430.

Rubin, L.L., Gatchalian, C.L., Rimon, G., Brooks, S.F., 1994. The molecular mechanisms of neuronal apoptosis. Curr. Opin. Neurobiol. 4, 696–702.

Sims, N.R., 1990. Rapid isolation of metabolically active mitochondria from rat brain and subregions using Percoll density gradient centrifugation. J. Neurochem. 55, 698–707.

Tang, D., Yeung, J., Lee, K.Y., Matsushita, M., Matsui, H., Tomizawa, K., Hatase, O., Wang, J.H., 1995. An isoform of the neuronal cyclin-dependent kinase 5 (Cdk5) activator. J. Biol. Chem. 270, 26897–26903.

Tsai, L.H., Takahashi, T., Caviness Jr., V.S., Harlow, E., 1993. Activity and expression pattern of cyclin-dependent kinase 5 in the embryonic mouse nervous system. Development 119, 1029–1040.

van den Heuvel, S., Harlow, E., 1993. Distinct roles for cyclin-dependent kinases in cell cycle control. Science 262, 2050–2054.

Vantieghem, A., Xu, Y., Assefa, Z., Piette, J., Vandenheede, J.R., Merlevede, W., De Witte, P.A., Agostinis, P. 2002. Phosphorylation of BCL-2 in G_2/M phase arrested cells following photodynamic therapy with hypericin involves a CDK1-mediated signal and delays the onset of apoptosis. J. Biol. Chem.

Walker, D., 1998. Small-molecule inhibitors of cyclin-dependent kinases: molecular tools and potential therapeutics. Curr. Top. Microbiol. Immunol. 227, 149–162.

Wüllner, U., Seyfried, J., Groscurth, P., Beinroth, S., Winter, S., Gleichmann, M., Heneka, M., Loschmann, P., Schulz, J.B., Weller, M., Klockgether, T., 1999. Glutathione depletion and neuronal cell death: the role of reactive oxygen intermediates and mitochondrial function. Brain Res. 826, 53–62.

Zukerberg, L.R., Patrick, G.N., Nikolic, M., Humbert, S., Wu, C.L., Lanier, L.M., Gertler, F.B., Vidal, M., Van Etten, R.A., Tsai, L.H., 2000. Cables links Cdk5 and c-Abl and facilitate Cdk5 tyrosine phosphorylation, kinase upregulation, and neurite outgrowth. Neuron 26, 633–646.